

Supporting Information

A Reversible Light-Operated Nanovalve on Mesoporous Silica Nanoparticles

*Derrick Tarn,[†] Daniel P. Ferris,^{†‡} Jonathan C. Barnes,[‡] Michael W. Ambrogio,[‡] J. Fraser
Stoddart[‡] and Jeffrey I. Zink^{*†}*

[†]Department of Chemistry and Biochemistry, California NanoSystems Institute,
University of California, Los Angeles, California 90095, United States

[‡]Department of Chemistry, Northwestern University, 2145 Sheridan Road,
Evanston, Illinois 60208-3113, United States

Table of Contents

Section A. Mesoporous Silica Nanoparticle Characterization	3
SI-1) <i>Transmission Electron Microscopy</i>	3
SI-2) <i>Powder X-Ray Diffraction</i>	4
SI-3) <i>Fourier Transform Infrared Spectroscopy</i>	5
Section B. Thread Characterization	6
SI-4) <i>¹HNMR Spectrum of 4,4'-Azobenzenecarboxylic acid</i>	6
SI-5) <i>¹HNMR Spectrum of 2</i>	7
SI-6) <i>¹HNMR Spectrum of 2b</i>	8
SI-7a) <i>¹HNMR Spectrum of 3a</i>	9
SI-7b) <i>ESI-TOF Mass Spectrum of 3a</i>	10
SI-8a) <i>¹HNMR Spectrum of 3b</i>	11
SI-8b) <i>ESI-TOF Mass Spectrum of 3b</i>	12
Section C. Thread-Modified Nanoparticle Characterization	13
<i>UV-Vis Spectroscopic Analysis</i>	
SI-9) <i>FRS1-MSN – Surface Functionalization</i>	13
SI-10) <i>EXT2-MSN – Surface Functionalization</i>	14
SI-11) <i>FRS1-MSN – Release of ARS</i>	15
Section D. Time-Resolved Spectroscopy	16
SI-11) <i>Experimental Setup for Time-Resolved Fluorescence Spectroscopy</i>	16
SI-12) <i>Continuous Fluorescence Monitoring of</i>	
<i>FRS1-MSN and EXT2-MSN</i>	17

Section A. Mesoporous Silica Nanoparticle Characterization

SI-1) *Transmission Electron Microscopy*

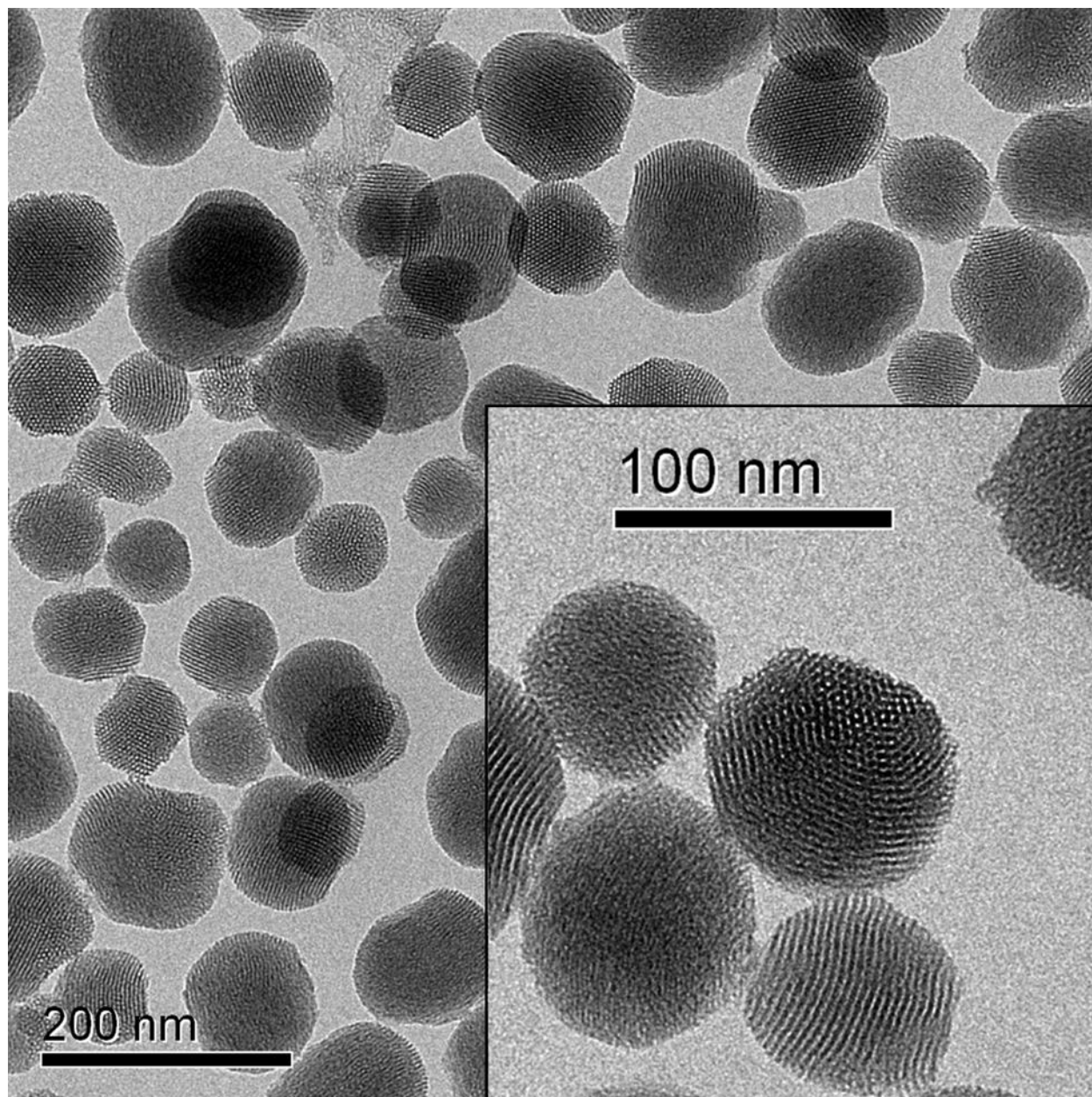


Fig. S1. TEM image of a typical batch of MCM-41 type nanoparticles showing the ordered, 2D hexagonal mesopore phase. In a typical batch, particles range from 80–120 nm in diameter, with an average pore size of 2.2 nm.

SI-2) Powder X-Ray Diffraction

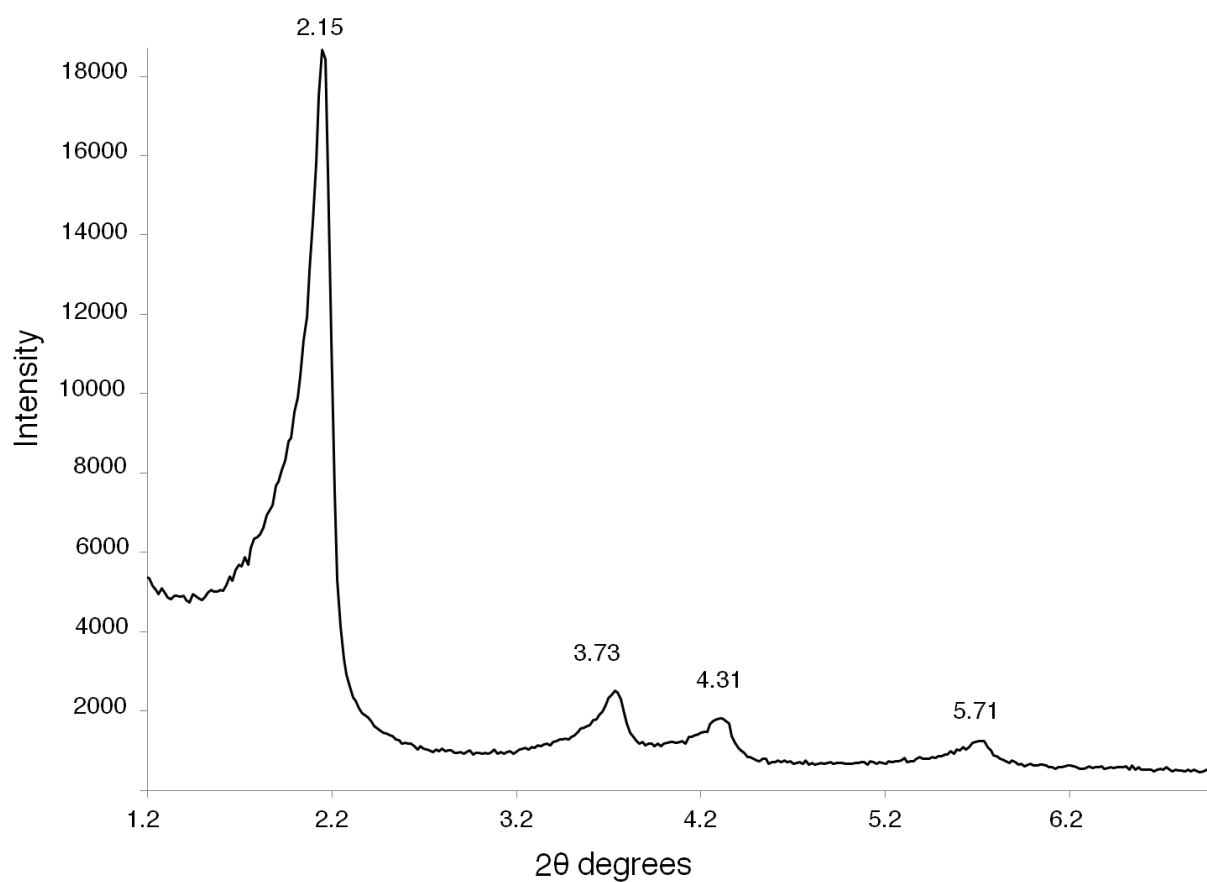


Fig. S2. Powder XRD of synthesized MCM-41 nanoparticles. The primary peak appears at 2.15, with a lattice spacing of 4 nm to give a calculated pore diameter of ~2 nm, in close agreement with TEM images of the synthesized nanoparticles.

SI-3) Fourier Transform Infrared Spectroscopy

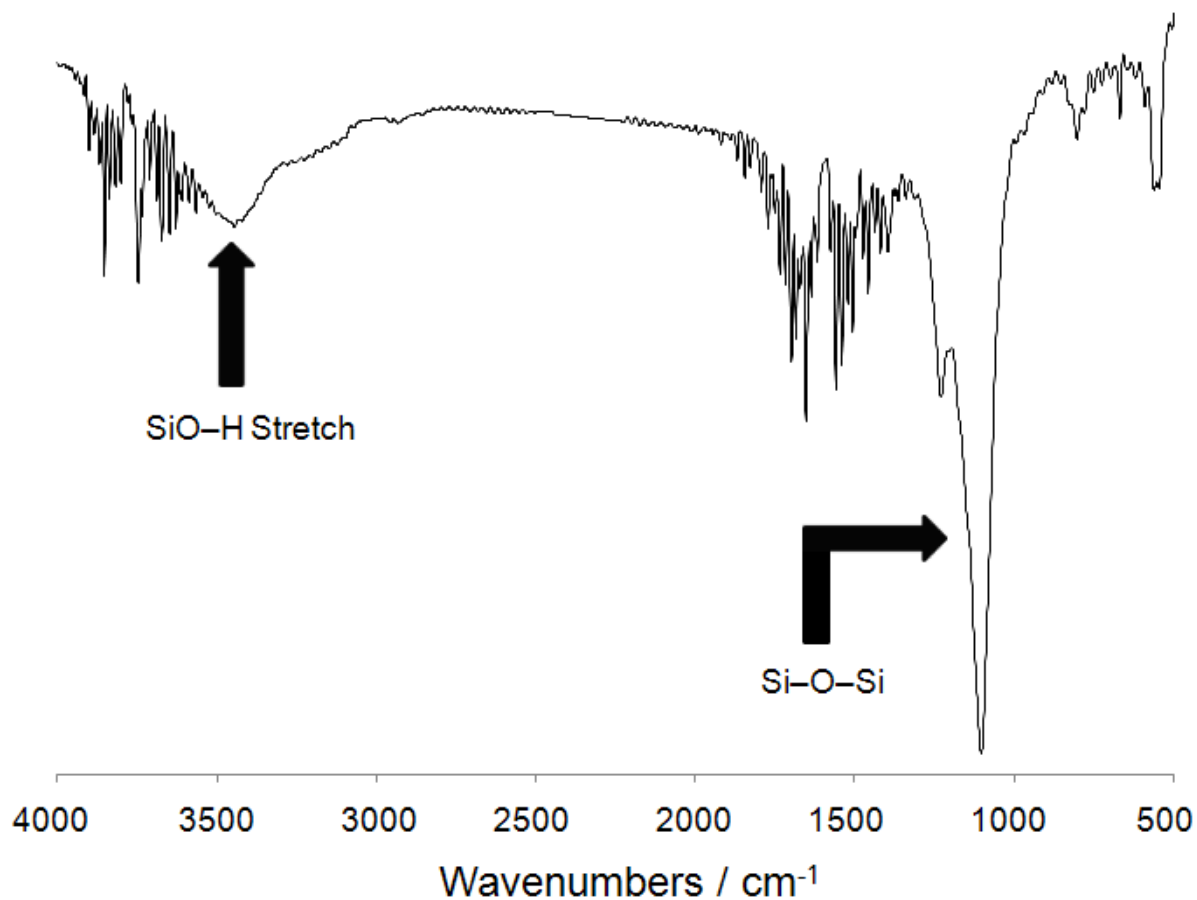


Fig. S3. FTIR spectrum of surfactant extracted MSN. The absence of C-H stretching bands at 3000 cm⁻¹ indicates complete removal of the surfactant templating agent CTAB.

Section B. Thread Characterization

SI-4) $^1\text{H-NMR}$ Spectrum of **1**

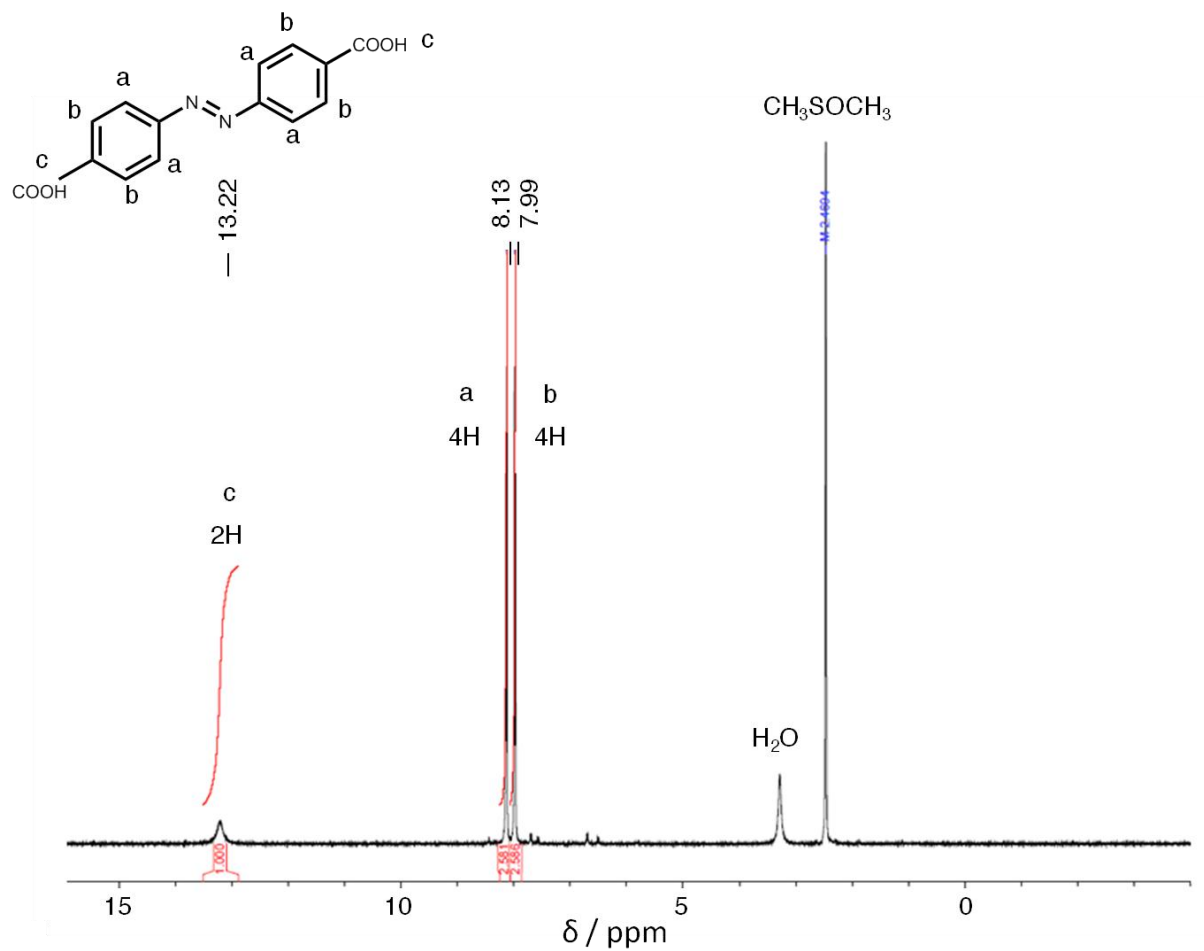


Fig. S4. $^1\text{H-NMR}$ spectrum of **1** in CD_3SOCD_3 .

SI-5) $^1\text{H-NMR}$ Spectrum of **2**

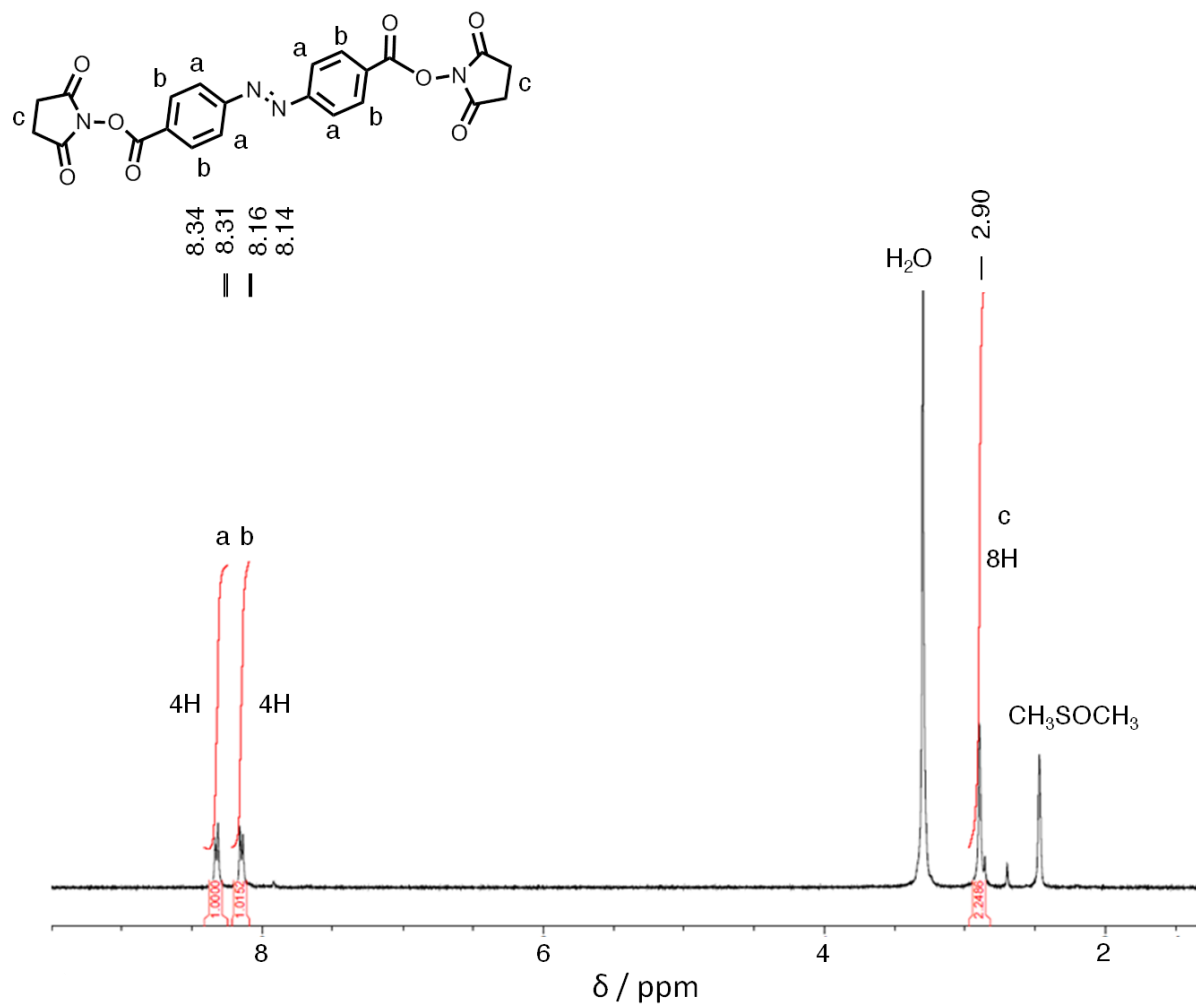


Fig. S5. $^1\text{H-NMR}$ spectrum of **2** in CD_3SOCD_3 .

SI-6) $^1\text{H-NMR}$ Spectrum of **2b**

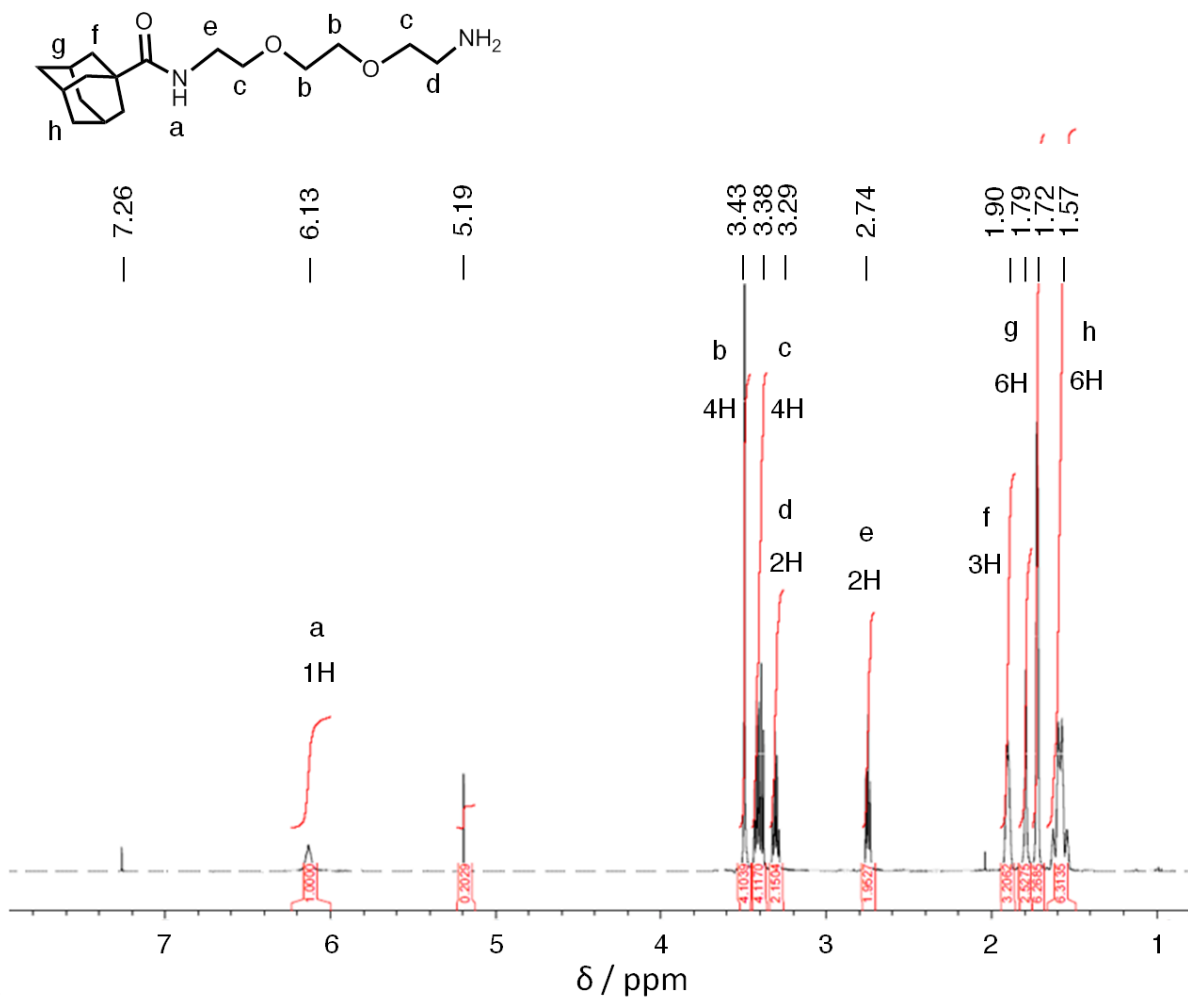


Fig. S6. $^1\text{H-NMR}$ spectrum of **2b** in CDCl_3 .

SI-7a) $^1\text{H-NMR}$ Spectrum of **3a**

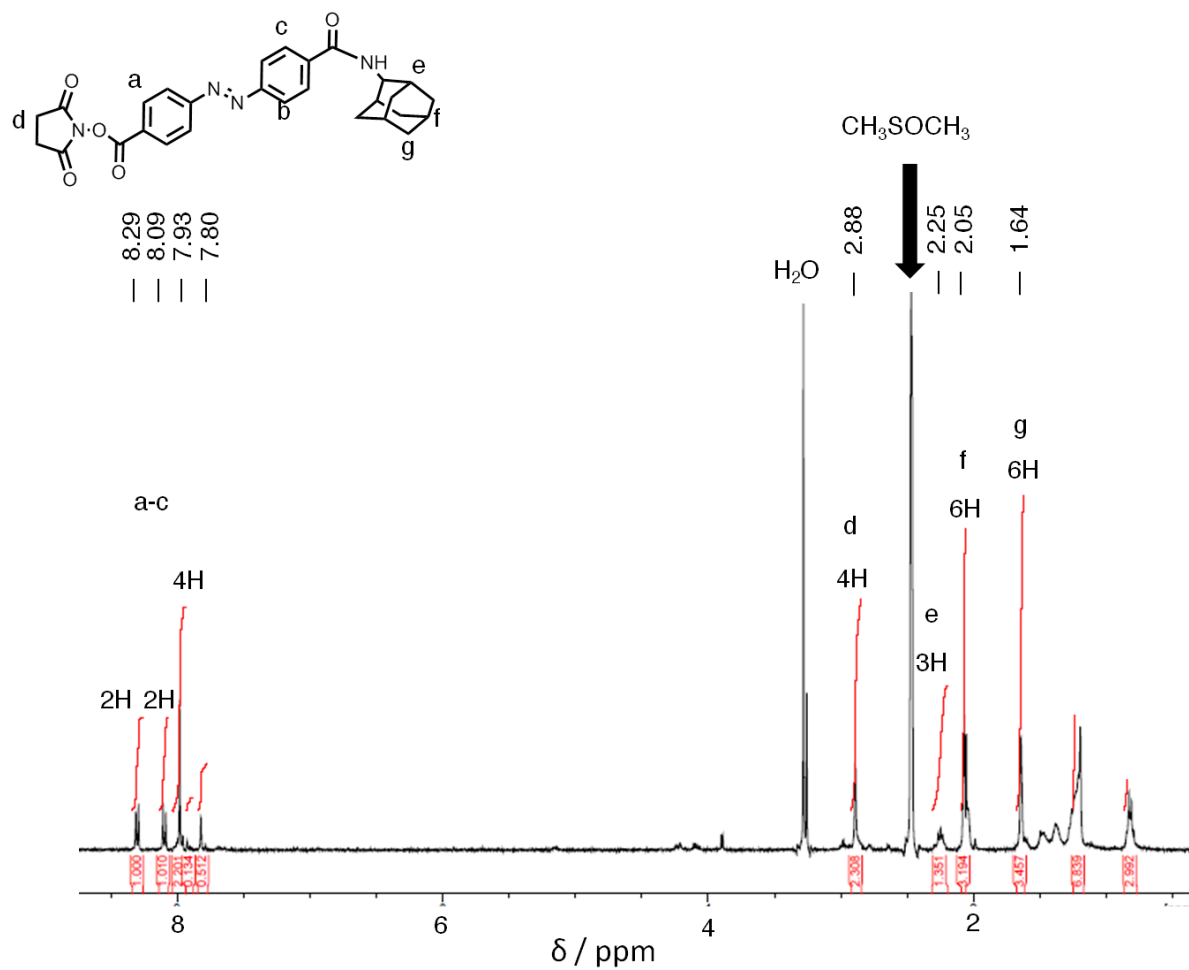


Fig. S7a. $^1\text{H-NMR}$ spectrum of **3a** in CD_3SOCD_3 .

SI-7b) ESI-TOF Mass Spectrum of 3a

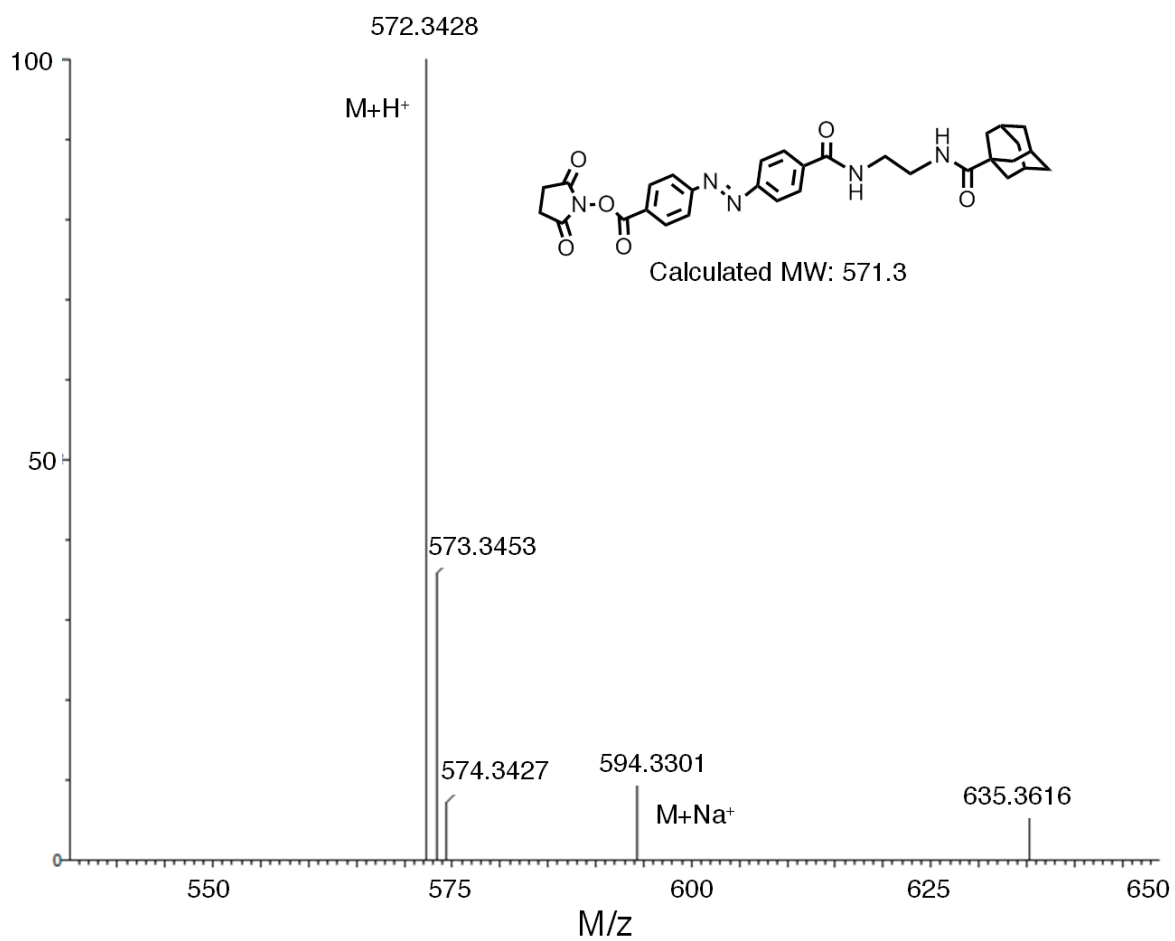


Fig. S7b. ESI-TOF mass spectrum of 3a.

SI-8a) $^1\text{H-NMR}$ Spectrum of **3b**

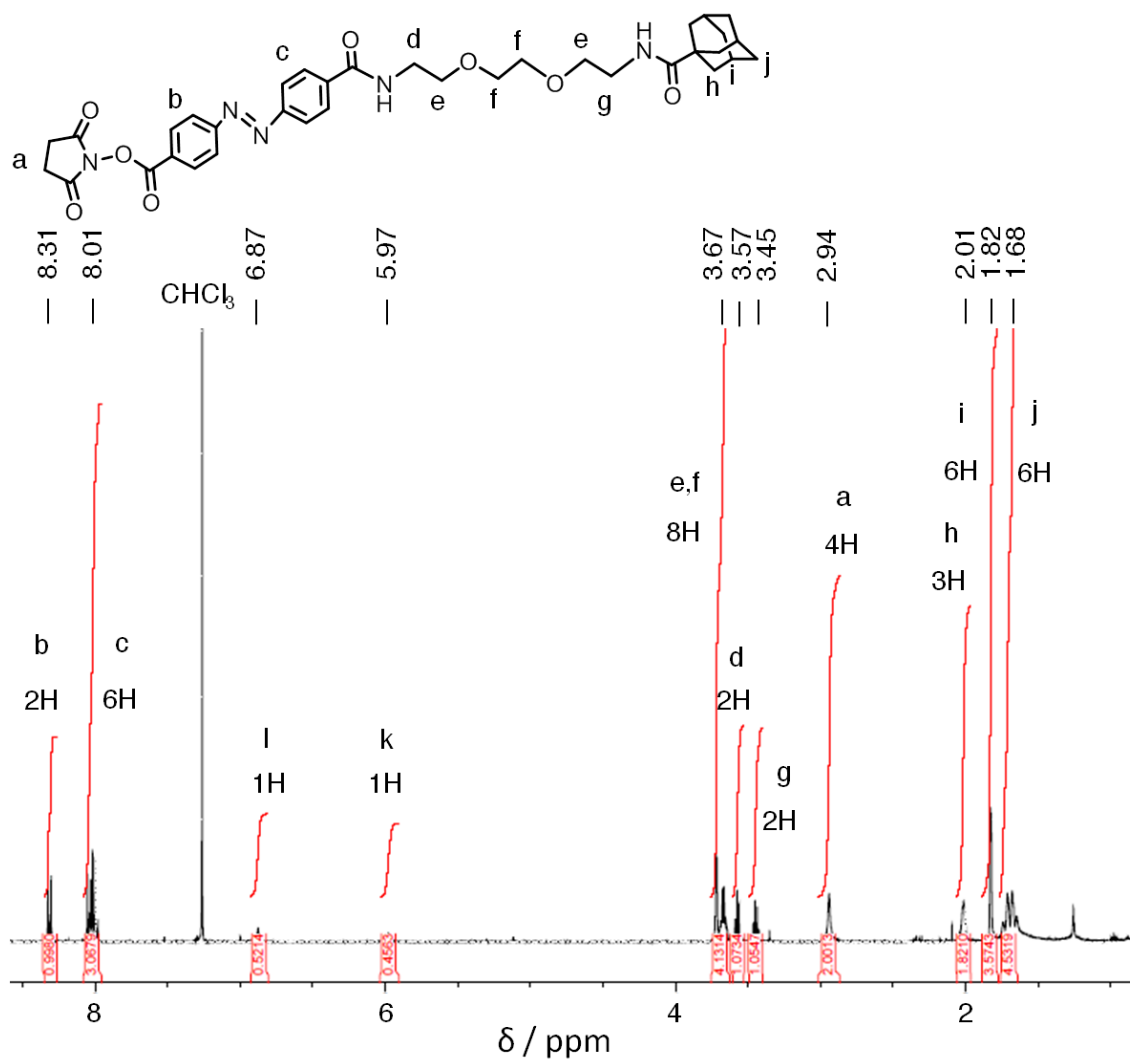


Fig. S8a. $^1\text{H-NMR}$ spectrum of **3b** in CDCl_3 .

SI-8b) ESI-TOF Mass Spectrum of 3b

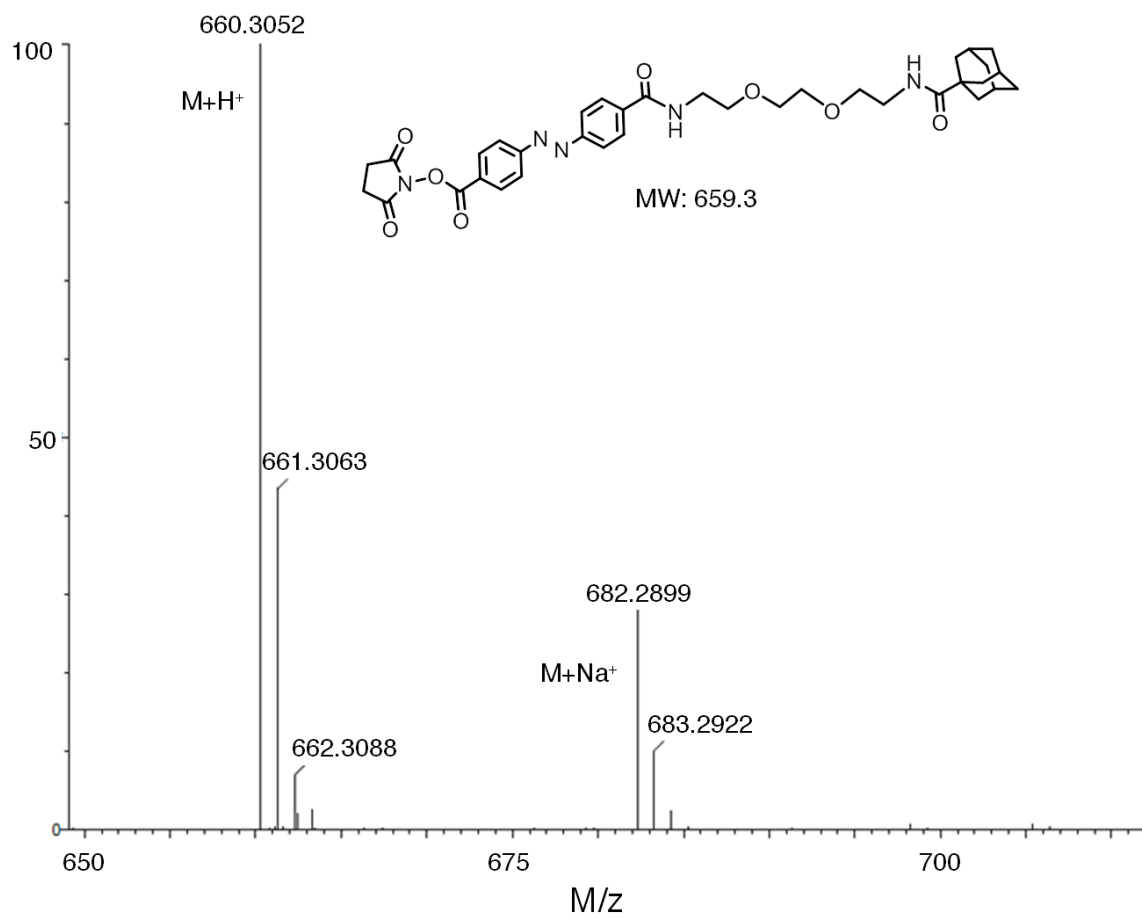


Fig. S8b. ESI-TOF mass spectrum of 3b.

Section C. Thread-Modified Nanoparticle Characterization

SI-9) UV-Vis Spectroscopic Analysis

a) *FRS1-MSN* – Surface Functionalization

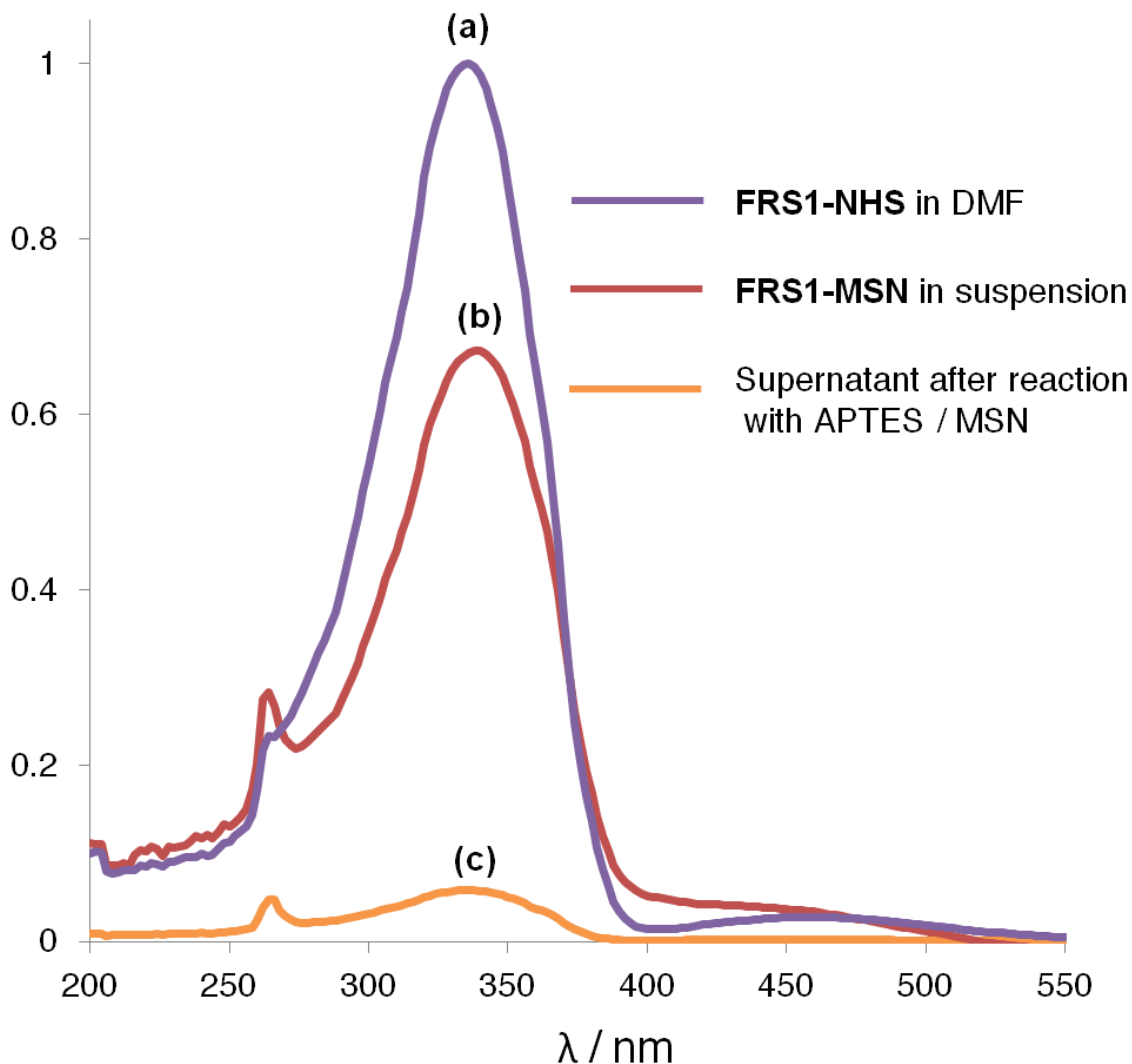


Fig. S9. UV-Vis absorption spectra proving successful reaction between Pseudorotaxane **FRS1-NHS** and APTES-modified MSN. Trace **(a)** shows the absorption of compound **FRS1-NHS** dissolved in DMF prior to reaction with APTES-modified MSN. After modification, an absorption spectrum of **FRS1-MSN** in suspension is shown in trace **(b)**. Finally, trace **(c)** shows the absorption of the supernatant solution after this attachment reaction has been completed, which indicates a successful reaction to attach the thread onto MSN. [All absorption spectra were normalized to trace **(a)**].

SI-10) *EXT2-MSN*

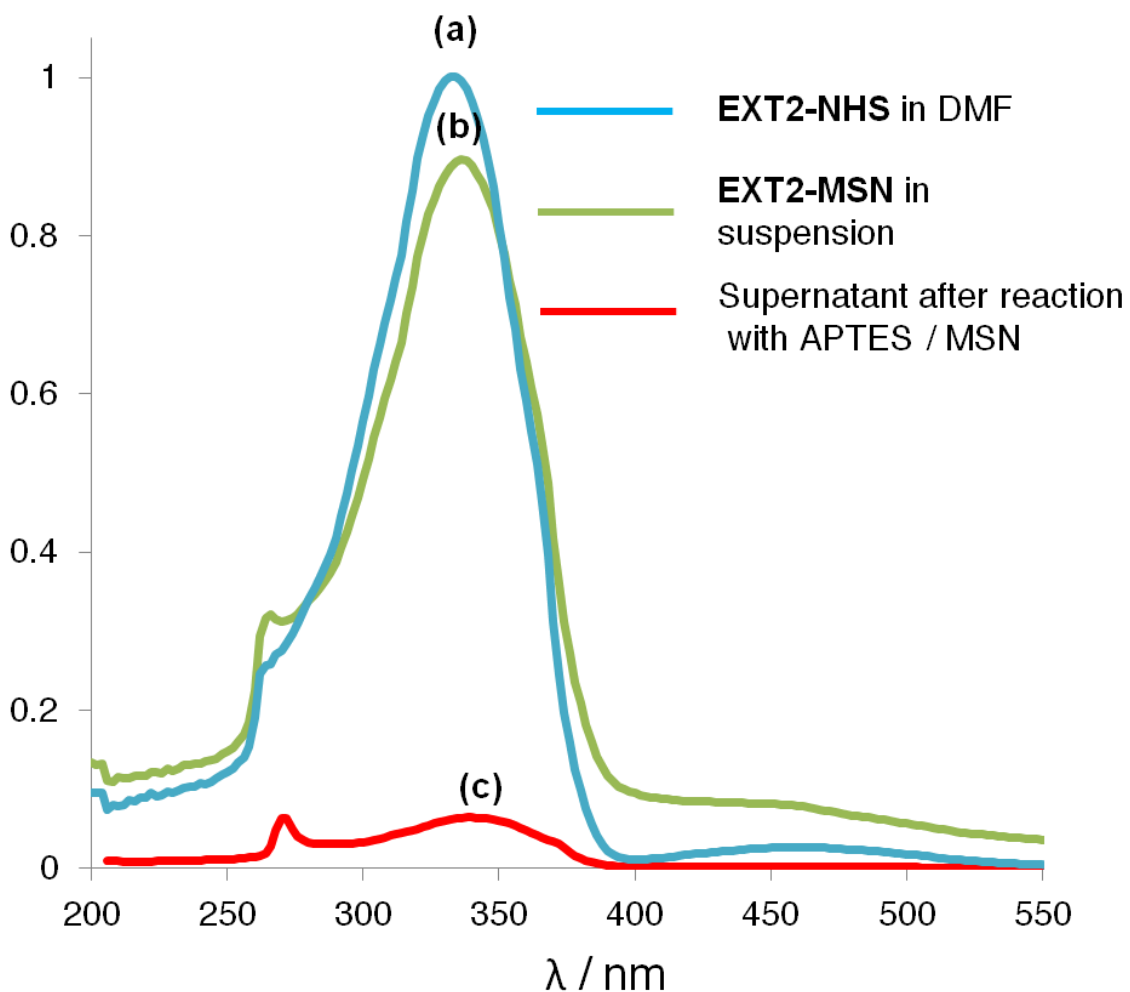


Fig. S10. UV-Vis absorption spectra proving successful reaction between **EXT2-NHS** and APTES-modified MSN. Trace **(a)** shows the absorbance of thread **EXT2-NHS** dissolved in DMF prior to reaction with APTES-modified MSN. Trace **(b)** shows the absorption of **EXT2-MSN** in suspension. Trace **(c)** shows the supernatant absorbance after the completed reaction, indicating that the thread has been successfully attached onto MSN. [All absorption spectra were normalized to trace **(a)**].

SI-11) *FRS1-MSN* – Release of ARS

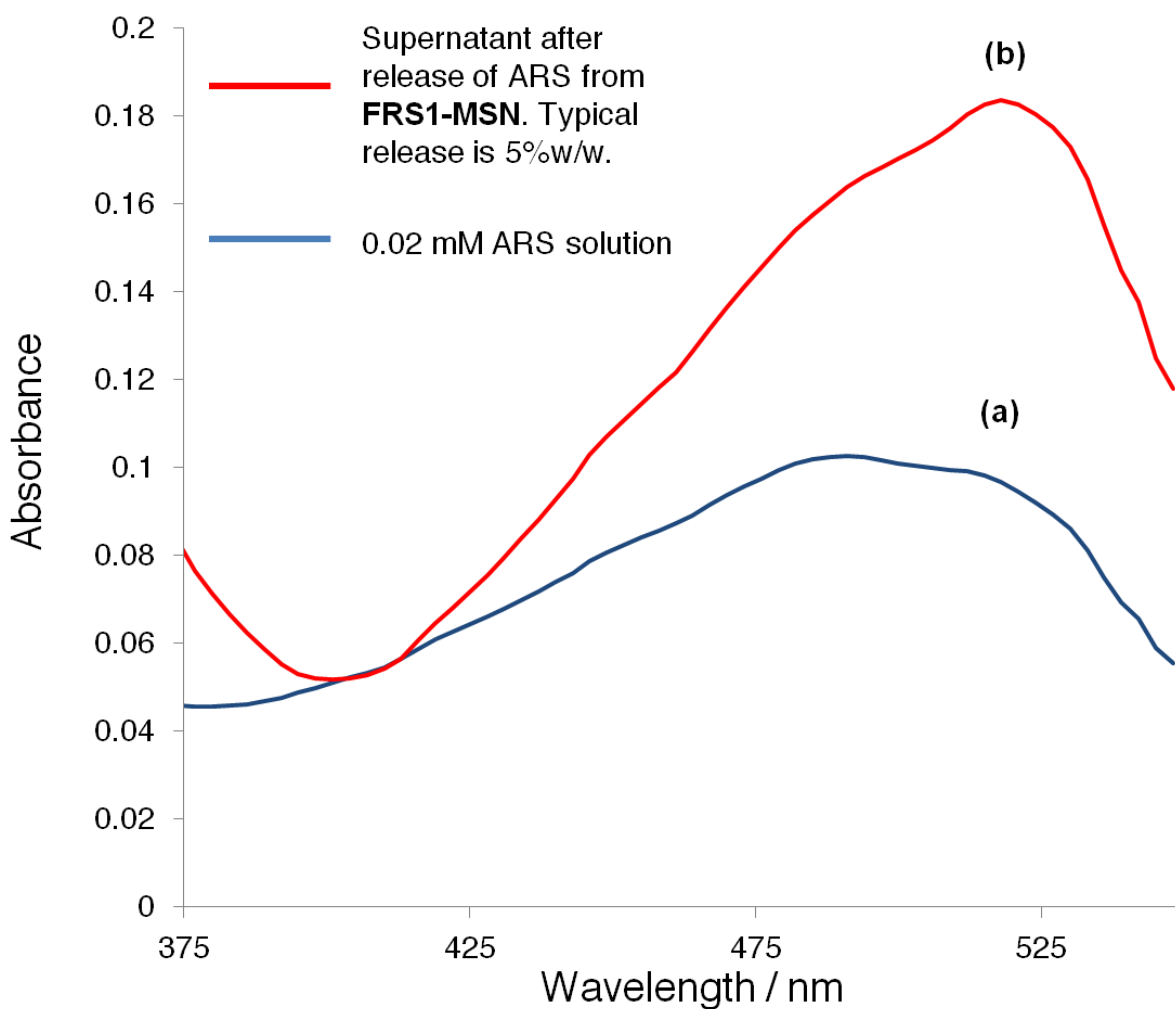


Fig. S11. UV-Vis absorption spectra of supernatant after release of ARS from **FRS1-MSN**. Trace **(a)** shows the absorbance of a 0.02 mM stock solution of ARS. Trace **(b)** shows the supernatant absorbance after a complete release from **FRS1-MSN**. Release weight percent was calculated from this trace to be 5% w/w.

Section D. Time-Resolved Spectroscopy

SI-12) Experimental Setup for Time-Resolved Fluorescence Spectroscopy

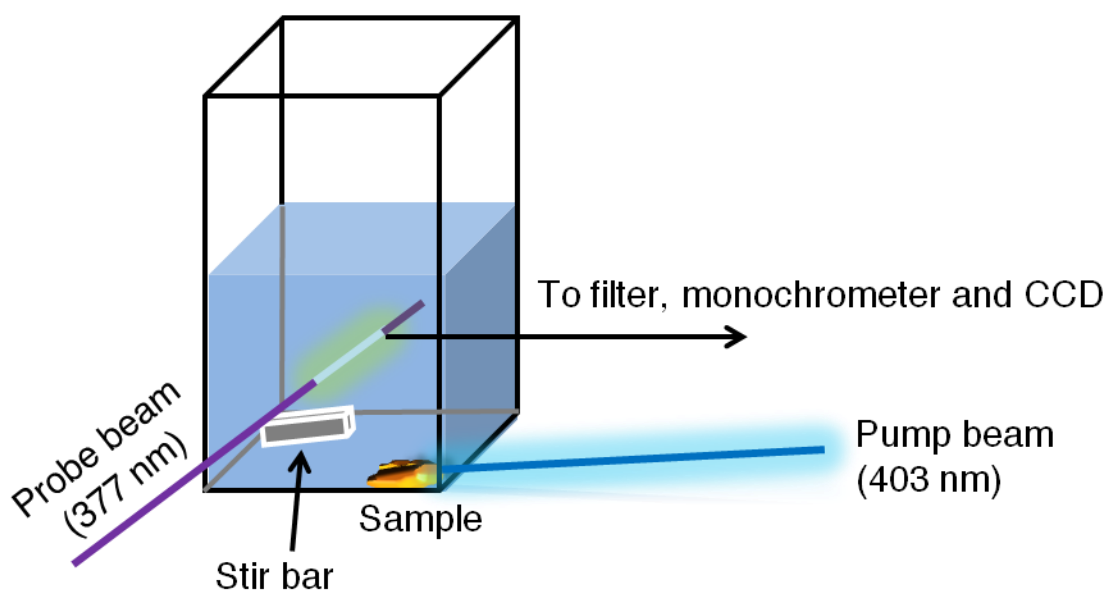


Fig. S12. Experimental setup for time-resolved fluorescence spectroscopy measurements. An excitation beam (377 nm, 1mW, 1 mm) is aimed at the solution supernatant, exciting any dye molecules present. The corresponding emission is passed through a cutoff filter, and a monochromator before being read on a CCD detector cooled to liquid nitrogen temperatures. Computer software integrates the intensities at a specified wavelength in real-time to generate a release profile. To initiate release, a pump beam (403 nm, 85 mW, 1 mm) is turned on and focused directly onto the sample to induce *trans*- to *cis*-azobenzene photoisomerization.

SI-13) Continuous Fluorescence Monitoring of FRS1-MSN and EXT2-MSN

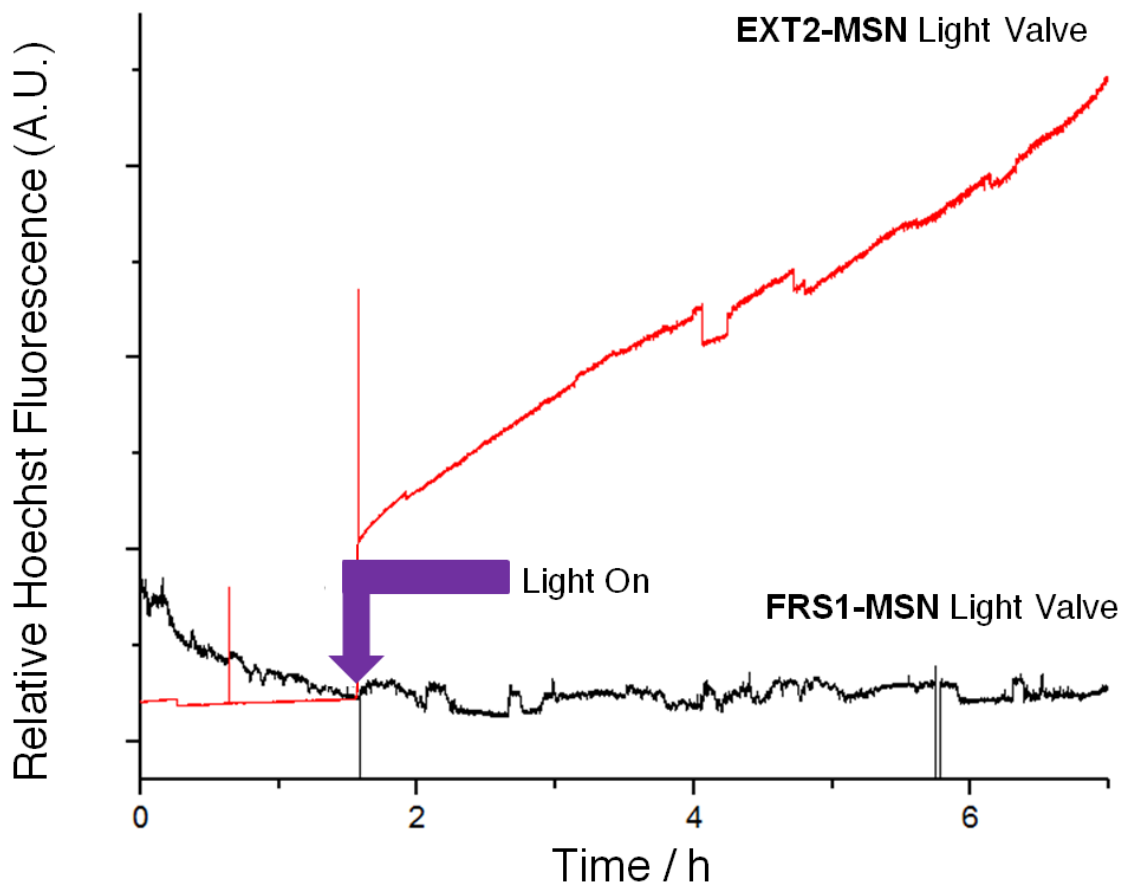


Fig. S13. Continuous fluorescence monitoring of **FRS1-MSN** loaded with Hoechst 33342 dye. No definite slope change is observed when the pump laser is turned on, indicating that this design cannot store and release larger cargo such as Hoechst, while **EXT2-MSN** shows a distinct fluorescence increase when irradiated.